

Investigation of Thermal Stability and Degradation Mechanisms in Ni-Based Ohmic Contacts to *n*-Type SiC for High-Temperature Gas Sensors

ARIEL VIRSHUP,^{1,4} LISA M PORTER,¹ DOROTHY LUKCO,²
KRISTINA BUCHHOLT,³ LARS HULTMAN,³ and ANITA LLOYD SPETZ³

1.—Carnegie Mellon University, Pittsburgh, PA, USA. 2.—ASRC Aerospace Corporation, Cleveland, OH, USA. 3.—Linköping University, Linköping, Sweden. 4.—e-mail: avirshup@andrew.cmu.edu

We investigated the thermal stability of Pt/TaSi_x/Ni/SiC ohmic contacts, which have been implemented in SiC-based gas sensors developed for applications in diesel engines and power plants. The contacts remained ohmic on lightly doped *n*-type ($\sim 1 \times 10^{16} \text{ cm}^{-3}$) 4H-SiC for over 1000 h in air at 300°C. Although a gradual increase in specific contact resistance from $3.4 \times 10^{-4} \Omega \text{ cm}^2$ to $2.80 \times 10^{-3} \Omega \text{ cm}^2$ was observed, the values appeared to stabilize after ~ 800 h of heating in air at 300°C. The contacts heated at 500°C and 600°C, however, showed larger increases in specific contact resistance followed by nonohmic behavior after 240 h and 36 h, respectively. Concentration profiles from Auger electron spectroscopy and electron energy-loss spectroscopy show that loss of ohmic behavior occurs when the entire tantalum silicide layer has oxidized.

Key words: Ohmic contacts, nickel contacts, semiconductor contacts, SiC contacts, degradation mechanism, stability, reliability

INTRODUCTION

With increasing attention being paid to curbing emission of pollutants into the atmosphere, chemical sensors that can be used to monitor and control these unwanted emissions are in great demand. Examples include monitoring of hydrocarbons from automobile engines and monitoring of flue gases such as CO emitted from power plants.

Because many of the polluting processes and gases require sensors that can be operated at high temperatures ($\sim 300^\circ\text{C}$ to 800°C) and in chemically aggressive environments, the intrinsic properties of SiC, such as its wide band gap and chemical inertness, give it substantial advantages for use in these sensors.^{1,2} Metal-insulator-silicon carbide sensors have been developed at the Swedish Sensor Centre (S-SENCE) and continues now at the Functional Nanoscale Materials, FunMat, Centre at Linköping

University in Sweden; the sensors can operate in an oxidizing ambient for short durations at temperatures up to 700°C .³

One of the critical limitations in high-temperature SiC gas sensors, however, is the degradation of the metal-SiC contacts over time. A review of thermal stability issues pertaining to ohmic contacts to SiC by Porter and Mohammad^{4,5} emphasizes the importance of selecting phases that are thermodynamically stable with each other at high temperatures, as it is thermodynamically favorable for SiC to react with most metals to form silicides and/or carbides at elevated temperatures. Further complications are introduced by the following additional requirements for high-temperature ohmic contacts: high resistance to oxidation, sufficient electrical conductivity, the ability to be connected to the external circuitry (e.g., wire bonding), and appropriate interfacial electrical properties (e.g., contact resistance or Schottky barrier height). In order to meet all of

(Received August 1, 2008; accepted December 1, 2008;
published online January 9, 2009)

these requirements, contact structures typically consist of multiple metal layers, any of which can introduce an additional thermodynamic instability to the system.

In this study, we investigated the high-temperature stability of Pt/TaSi_x/Ni/SiC ohmic contacts, which have been implemented in actual SiC-based gas sensors developed for applications in diesel engines and power plants.^{6,7} The specific contact resistance, interfacial chemistry, and surface morphology were characterized as a function of thermal treatment time in air at 300°C, 500°C, and 600°C. The evidence presented here offers an explanation of the primary degradation mechanisms that are responsible for electrical failure of the ohmic contacts at high temperatures.

EXPERIMENTAL PROCEDURE

Single-crystal *n*-type 4H-SiC substrates were used for all of the studies in this research. The devices were fabricated on a *N*-doped substrate ($\sim 5 \times 10^{16} \text{ cm}^{-3}$) containing a 1- μm -thick *n*-type epitaxial layer with a nitrogen doping concentration of $1 \times 10^{16} \text{ cm}^{-3}$, as determined by secondary-ion mass spectroscopy analysis. The fabrication and processing of the devices were performed at ACREO AB, Stockholm, Sweden and Linköping University. First, a 100-nm-thick Ni layer was deposited by thermal evaporation. Since as-deposited Ni contacts to *n*-type SiC are typically rectifying,⁸ a 5-min anneal was performed in Ar at 950°C to form ohmic contacts (the short-term, high-temperature annealing step is normally required to produce ohmic contacts on low and moderately doped epilayers of both *n*- and *p*-type SiC).⁹ Subsequently, a 50-nm-thick TaSi_x adhesion layer and a 150-nm-thick Pt capping layer were deposited by magnetron sputtering. Linear transfer length method (TLM) patterns, along with sensor devices (not used in this study), were fabricated using traditional photolithographic techniques; the former devices were used for calculations of specific contact resistivity. The TLM contact patterns consisted of $150 \mu\text{m} \times 500 \mu\text{m}$ rectangles with the following contact spacings: 10 μm , 20 μm , 30 μm , 40 μm , and 50 μm . Each set of TLM patterns was isolated from one another by mesas.

Thermal stability tests were conducted using a tube furnace to heat the samples to 300°C, 500°C, or 600°C in a flow of synthetic air for varying intervals of time. After the samples cooled to room temperature, current–voltage measurements were performed and images of the metal surfaces were obtained with a scanning electron microscope (SEM). The series of thermal treatments was terminated if the contacts became nonohmic. Auger electron spectroscopy (AES) depth profiles were obtained from selected samples to observe the interfacial chemistry. Additional materials characterization included transmission electron

microscopy (TEM) with electron energy-loss spectroscopy (EELS). The TEM cross-section specimens were prepared by a technique that uses a focused ion beam system, equipped with SEM, to cut out and polish the desired section of the contact.

RESULTS AND DISCUSSION

A summary of the electrical results is given in Fig. 1, which shows a plot of the average specific contact resistance as a function of time for each test temperature. The contacts that underwent thermal treatments in air at 300°C displayed ohmic behavior throughout the 1000-h test. The specific contact resistance increased slowly from $3.44 \times 10^{-4} \Omega \text{ cm}^2$ before heating to $2.80 \times 10^{-3} \Omega \text{ cm}^2$ after 1000 h of heating in air at 300°C. We note that the absolute contact resistance values are expected to be relatively high because of the low doping concentration of the SiC substrate, which was designed primarily for the sensor devices. The values reported here are comparable to others reported for Ni ohmic contacts to SiC with similar doping levels and ohmic contact anneal conditions.^{10,11} Furthermore, it is not the absolute values of contact resistance that are important in this study; rather, it is the change in the values as a function of time and temperature that we sought to monitor. In the case of heating at 300°C, the contact resistance appears to stabilize after approximately 800 h.

However, Fig. 1 shows that the contacts become electrically unstable when tested in air at 500°C or 600°C. When heated at 500°C, the specific contact resistance increased dramatically from $2.56 \times 10^{-4} \Omega \text{ cm}^2$ before heating in air to $6.60 \times 10^{-2} \Omega \text{ cm}^2$ after 200 h of heat treatment. These contacts were no longer ohmic after 240 h at 500°C. We note that these contacts remained ohmic longer than similar contacts reported in a previous study.¹² The difference

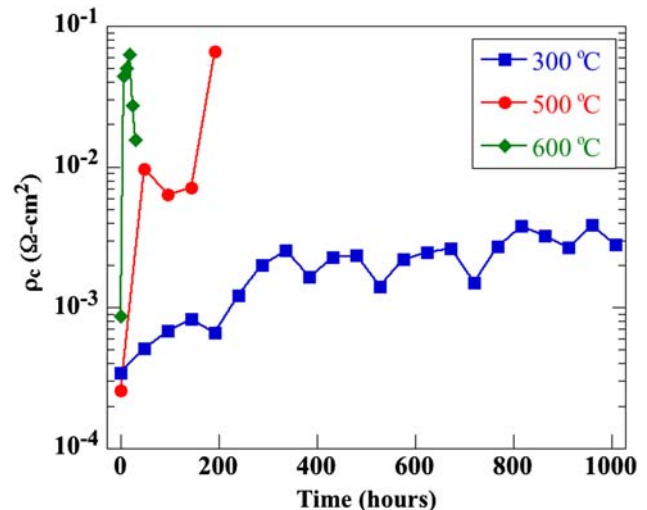


Fig. 1. Average specific contact resistance of Pt/TaSi_x/Ni/SiC as a function of time at 300°C, 500°C, and 600°C, determined from current–voltage measurements that were taken at room temperature, after cooling the samples.

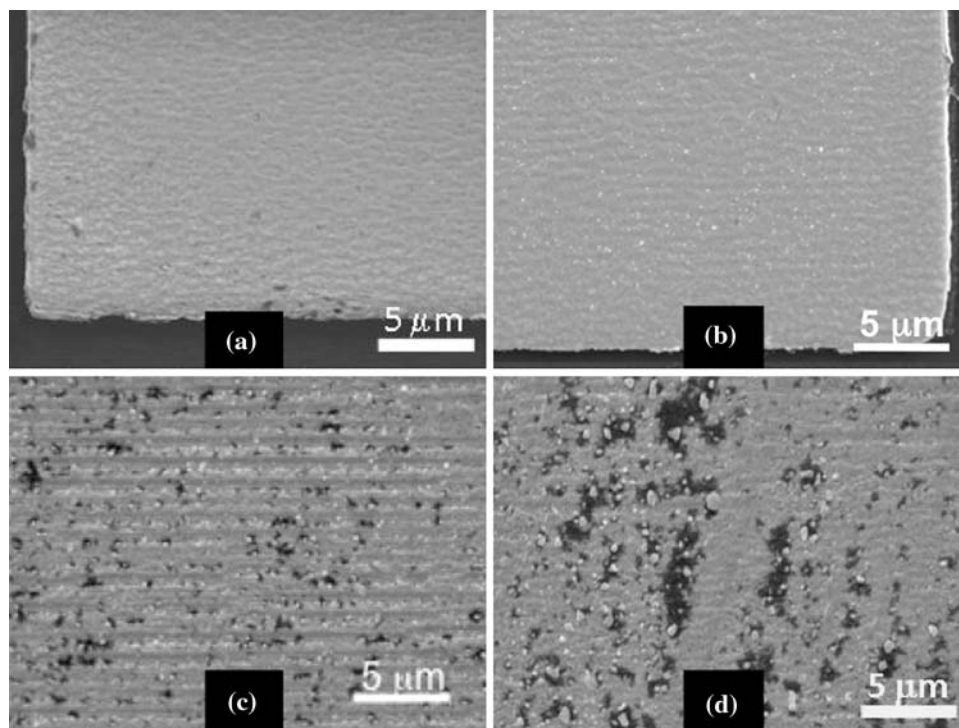


Fig. 2. SEM images of the surfaces of (a) as-received contacts and contacts that were heated in air at (b) 300°C for 1000 h, (c) 500°C for 240 h, and (d) 600°C for 48 h.

may be due to a difference in the Pt layer thickness, slightly different processing conditions, and different testing conditions (e.g., electrical measurements conducted at elevated versus room temperature).

The sample heated at 600°C was not ohmic after the first 48-h interval, so a separate sample was tested and characterized after shorter (6-h) time intervals. This sample became nonohmic after 36 h of 600°C heat treatment in air.

The changes in surface morphology after heating at each temperature are revealed by the SEM images in Fig. 2. No significant change was observed after 1000 h of heating in air at 300°C. However, discontinuities in the contacts were observed after 240 h at 500°C and after 48 h at 600°C. As reported above, these contacts (Fig. 2c and d) were no longer ohmic. Our observations led us to investigate the microstructural and chemical details within the similar morphological structures that developed in these failed contacts.

Auger depth profiles were used to monitor the locations of the primary elemental constituents at selected points of the series of thermal treatments in air. The depth profile of the as-received contact (after the ohmic contact anneal, of Ni/SiC, which resulted in the formation of Ni-silicide and free carbon, Fig. 3a) shows some O at the interface between the Ni and TaSi_x layers; this result is attributed to oxygen accumulation in between the Ni ohmic contact anneal and subsequent TaSi_x/Pt depositions. A contact that was still performing well electrically (heated at 300°C for 288 h) was also analyzed.

The AES profile in Fig. 3b shows that oxygen diffused into the contact during the heat treatment and is located primarily at the Pt/TaSi_x and TaSi_x/Ni_ySi_z interfaces. The interfacial oxygen accumulation may be responsible for the increase in the specific contact resistance of this sample (Fig. 1).

The AES depth profile in Fig. 3c was obtained from a sample that had failed electrically (heated at 500°C for 240 h). In this case, the oxygen no longer resides exclusively at the metal–metal interfaces but exists throughout the Ta silicide layer. Moreover, we observed oxidation of the TaSi_x layer to a greater extent in a different sample that was analyzed well after failure (heated at 600°C for 48 h, Fig. 3d). Complete oxidation of the TaSi_x layer could account for the loss of ohmicity, because the tantalum oxides are electrically insulating (resistivities between 10¹¹ Ω cm and 10¹⁷ Ω cm).¹³

In addition to the oxygen content, the presence of free carbon in the contact structure is of concern. Some as-received contacts peeled off during solvent cleaning. A depth profile for one of these contacts (not shown) revealed that the contact peeled at the TaSi_x/Ni_ySi_z interface. High carbon content at the exposed surface suggests that the poor adhesion is related to the “free” carbon remaining from the reaction between Ni and SiC.

Cross-sectional TEM images and EELS analyses provide additional information on the morphology and composition of contacts before and after the thermal treatments in air. The combination of imaging and EELS data allows us to determine the

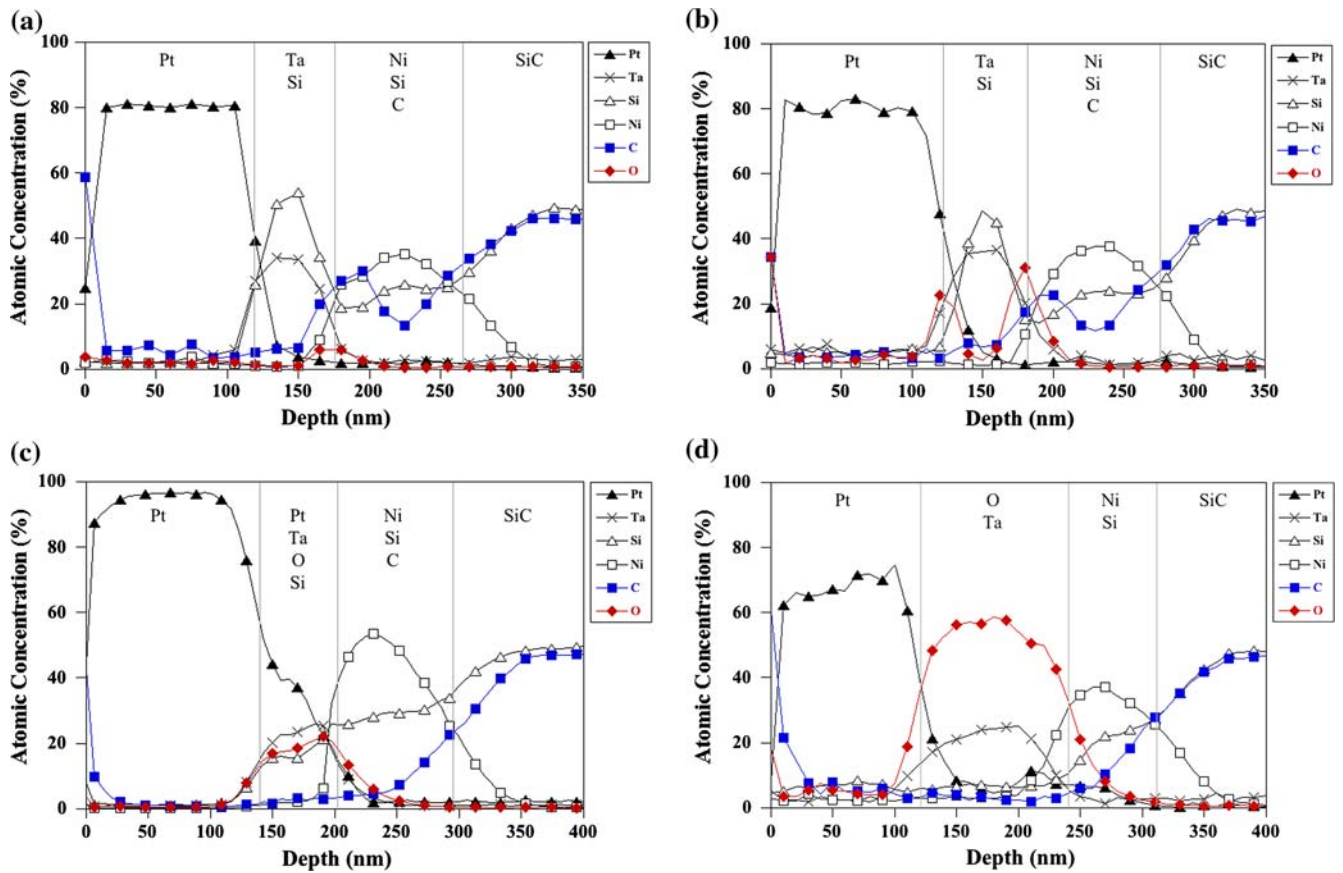


Fig. 3. AES depth profiles of (a) an as-received contact; and contacts heated in air (b) at 300°C for 288 h, (c) at 500°C for 240 h, and (d) at 600°C for 48 h.

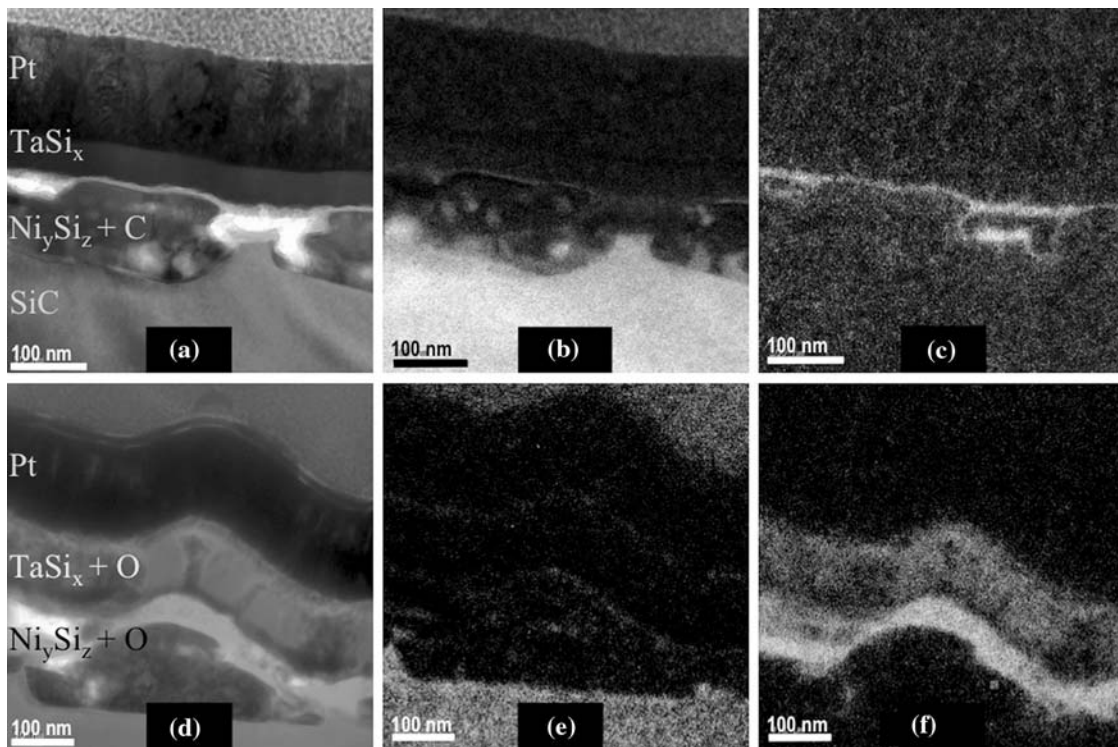


Fig. 4. Reference images (a, d) and corresponding EELS maps indicating carbon (b, e) and oxygen (c, f) in cross sections of an as-received contact (top) and a contact heated in air at 600°C for 36 h (bottom).

primary elemental constituents of the layers, which are labeled Fig. 4a and d. From these images it is apparent that the initial morphology was quite smooth; however, the failed contact (600°C/36 h) shows an undulating morphology. The EELS maps, showing the presence of carbon (b, e) and oxygen (c, f) in white contrast, correspond with the TEM reference images for the as-received (a) and heat-treated (d) contacts, respectively. Complete oxidation of the Ta silicide layer is clearly observed in the heat-treated sample, which agrees with the AES results discussed above. Interestingly, virtually no carbon was detected in the heat-treated sample. We propose that the migration and eventual loss of carbon that was freed up by the nickel silicide reaction is associated with the oxidation that occurs initially at the metal layer interfaces and may provide a rapid pathway for oxygen to diffuse into the contacts. A similar process was suspected to occur in Pt/TaSi₂/Ti/SiC contacts reported by Okojie et al.¹⁴; they reported that Ti outdiffusion allowed oxygen to diffuse to the Ti/SiC interface.

SUMMARY

Pt/TaSi_x/Ni/SiC ohmic contacts were characterized before and after heat treatments in air at 300°C, 500°C, and 600°C. The contacts heated at 300°C remained ohmic and exhibited relatively stable electrical characteristics after heating for 800 h. The contacts heated at 500°C were not ohmic after 240 h, whereas contacts heated at 600°C failed after 36 h. Chemical analyses revealed an increasing amount of oxygen at the metal layer interfaces with increasing temperature and time. We concluded that complete oxidation of the tantalum silicide layer is responsible for electrical failure of the ohmic contacts. We also propose that the loss of C during the long-term heat treatments may facilitate oxidation of the interfaces and ultimately throughout the tantalum silicide layer.

ACKNOWLEDGEMENTS

The research at Carnegie Mellon was supported by the National Science Foundation under Award

No. DMR-0304508 and by the Pennsylvania Infrastructure Technology Alliance. Metal films in this study were grown using equipment funded by the National Science Foundation (Grant# DMR-9802917). Additional grants are acknowledged from the Swedish Research Council, the Swedish Governmental Agency for Innovation Systems and Swedish Industry.

REFERENCES

1. A. Lloyd Spetz and S. Savage, *Recent Major Advances in SiC*, ed. W.J. Choyke, H. Matsunami, and G. Pensl (Berlin, Germany: Springer, 2003), pp. 879–906.
2. G.W. Hunter, P.G. Neudeck, J. Xu, D. Lukco, A. Trunek, M. Artale, P. Lampard, D. Androjna, D. Makel, B. Ward, and C.C. Liu, *Mater. Res. Soc. Symp. Proc.* 815, J4.4.1 (2004).
3. H. Wingbrant, H. Svenningstorp, P. Salomonsson, P. Tengström, I. Lundström, and A.L. Spetz, *Sens. Actuators B. Chem.* 93, 295 (2003). doi:10.1016/s0925-4005(03)00227-2.
4. L.M. Porter and F.A. Mohommad, *SiC MEMS for Harsh Environments*, ed. R. Cheung (London, UK: Imperial College Press, 2006).
5. L.M. Porter, *Wide Band Gap Materials and New Developments*, ed. M. Syvajarvi and R. Yakimova (Kerala, India: Research Signpost, 2006).
6. H. Wingbrant, H. Svenningstorp, P. Salomonsson, D. Kubinski, J.H. Visser, M. Löfdahl, and A.L. Spetz, *IEEE Sens. J.* 5, 1099 (2005). doi:10.1109/JSEN.2005.854489.
7. M. Andersson, L. Everbrand, A. Lloyd Spetz, T. Nyström, M. Nilsson, C. Gauffin, and H. Svensson, *Proc. IEEE Sensors*, October 28–31, 2007, Atlanta, USA, pp. 962–965.
8. J.R. Waldrop and R.W. Grant, *Appl. Phys. Lett.* 62, 2685 (1993). doi:10.1063/1.109257.
9. L.M. Porter and R.F. Davis, *Mater. Sci. Eng. B* B34, 83 (1995). doi:10.1016/0921-5107(95)01276-1.
10. B. Barda, P. Machac, M. Hubičková, and J. Náhlík, *J. Mater. Sci. Mater. Electron.* 19, 1039 (2008). doi:10.1007/s10854-007-9446-7.
11. G. Kelner, S. Binani, M. Shur, and J.W. Palmour, *Electron. Lett.* 27, 1038 (1991). doi:10.1049/el:19910646.
12. S.-K. Lee, E.-K. Suh, N.-K. Cho, H.-D. Park, L. Uneus, and A.L. Spetz, *Solid State Electron.* 49, 1297 (2005). doi:10.1016/j.sse.2005.06.005.
13. S. Ezhilvalavan and T.Y. Tseng, *J. Mater. Sci. Mater. Electron.* 10, 9 (1999). doi:10.1023/A:1008970922635.
14. R.S. Okojie, D. Lukco, Y.L. Chen, and D.J. Spry, *J. Appl. Phys.* 91, 6553 (2002). doi:10.1063/1.1470255.